Analysis and Design Trade-Offs for Power Network Inter-Area Oscillations

Xiaofan Wu, Florian Dörfler, and Mihailo R. Jovanović

Abstract— **Conventional analysis and control approaches to inter-area oscillations in bulk power systems are based on a modal perspective. Typically, inter-area oscillations are identified from spatial profiles of poorly damped modes, and they are damped using carefully tuned decentralized controllers. To improve upon the limitations of decentralized controllers, recent efforts aim at distributed wide-area control strategies that involve the communication of remote signals, which are typically chosen to maximize modal observability metrics. Here, we investigate a novel approach to the analysis and control of inter-area oscillations. Our framework is based on a stochastically driven system with performance outputs chosen such that the $\mathcal{H}_2$ norm is associated to incoherent inter-area oscillations. We show that an analysis of the output covariance matrix offers new insights complementary to modal approaches. Next, we leverage the recently proposed sparsity-promoting optimal control approach to design controllers that simultaneously optimize the closed-loop performance and the control architecture. We investigate various performance trade-offs between fully decentralized and distributed wide-area controllers. In the end, we are able to identify decentralized control architectures that are capable of reasonable performance levels compared to the optimal centralized controllers.**

I. Introduction

Inter-area oscillations in bulk power systems are associated with the dynamics of power transfers and involve groups of synchronous machines oscillating relative to each other. These system-wide oscillations arise from modular network topologies (with tightly clustered groups of machines and sparse interconnections among these clusters), heterogeneous machine dynamics (resulting in slow and fast responses), and large inter-area power transfers further promoting oscillations. As the system loading increases and renewables are deployed in remote areas, long-distance power transfers will outpace the addition of new transmission facilities. As a result, inter-area oscillations become ever more weakly damped, induce severe stress and performance limitations on the transmission network, and may even become unstable and cause outages [1], see the 1996 Western U.S. blackout [2].

Traditional analysis and control approaches to inter-area oscillations are based on modal approaches [3], [4]. Typically, inter-area oscillations are identified from the spatial profiles of eigenvectors and participation factors of poorly damped modes [5], [6]. Such oscillations are conventionally damped via decentralized controllers, whose gains are carefully tuned according to root locus criteria [7]–[9].

To improve upon the limitations of decentralized controllers, recent research efforts aim at distributed wide-area control strategies that involve the communication of remote signals, see the surveys [10], [11] and the excellent articles in [12]. The wide-area control signals are typically chosen to maximize modal observability metrics [13], [14], and the control design methods range from root locus criteria to robust and optimal control approaches [15]–[17].

Here, we investigate a novel approach to the analysis and control of inter-area oscillations. Our unifying analysis and control framework is based on a stochastically driven power system model with performance outputs inspired by slow coherency theory [18], [19]. We analyze inter-area oscillations by means of the $\mathcal{H}_2$ norm of this system, as in recent related approaches for interconnected oscillator networks and multi-machine power systems [20]–[22]. We show that an analysis of power spectral density and variance amplification offers new insights that complement conventional modal approaches.

To identify a suitable and sparse wide-area control architecture and to design optimal controllers, we appeal to the recently proposed paradigm of sparsity-promoting optimal control [23]–[26]. Sparsity-promoting control approaches have been successfully employed in power system wide-area control problems [27]–[31]. Here, we follow the sparsity-promoting optimal control framework developed in [24], [29] and find a linear static state feedback that simultaneously optimizes a standard quadratic $\mathcal{H}_2$ optimal control criterion (associated to incoherent and poorly damped inter-area oscillations) and induces a sparse control architecture. We investigate different performance indices resulting in controllers that strike a balance between low communication complexity and closed-loop performance. We are able to identify fully decentralized controllers that achieve comparable performance relative to the optimal centralized controllers. Thus, our results also provide a constructive answer to the much-debated question whether locally observable oscillations in a power network are also locally controllable; see [32]. We illustrate the utility of our approach with the IEEE 39 New England power grid model, whose data can be found in [33].

The remainder of this paper is organized as follows. In Section II-A, we recall the modeling and causes for inter-area oscillations in power networks. In Section II-B, we introduce a new perspective of analysis and control of

Financial support from the National Science Foundation under award CMMI-09-27720, from the University of Minnesota Initiative for Renewable Energy and the Environment under Early Career Award RC-0014-11 and from University of California, Los Angeles Electrical Engineering Department start-up funds is gratefully acknowledged.

Xiaofan Wu and Mihailo R. Jovanović are with the Department of Electrical and Computer Engineering, University of Minnesota, Minneapolis, MN 55455. Email: [wuxxx836,mihailo]@umn.edu. F. Dörfler is with the Department of Electrical Engineering at the University of California Los Angeles, Los Angeles, CA. Email: dorfler@seas.ucla.edu

inter-area oscillations, power spectral density and variance amplification analysis. In Section II-C, we formulate the sparsity-promoting optimal control problem subject to structural constraints. In Section III, we present our control design and analysis for the IEEE 39 New England power grid. Finally, Section IV concludes the paper.

II. Problem formulation

A. Modeling and background on inter-area oscillations

A power network is described by the nonlinear dynamics of generators and their control equipments as well as the algebraic load flow, generator stator, and power electronic circuit equations [34]. After linearizing the dynamics around a stationary operating point and eliminating the algebraic equations, we obtain a linear state space model of the form

$$\dot{x} \;=\; A\,x \;+\; B_1\,d \;+\; B_2\,u\,, \tag{1}$$

where x is the state, u is the control action provided by generator excitation/governor control or power electronics control devices, and d represents disturbance in the form of white-noise, for example, from fluctuations in generation and loads [34], [35].

When neglecting the fast electrical dynamics as well as control and disturbance inputs, the dominant dynamic behavior of a multi-machine power system arises from the electro-mechanical dynamics among the generators, which are typically modeled by the *swing equations* [34]:

$$M\,\ddot{\theta} \;+\; D\,\dot{\theta} \;+\; L\,\theta \;=\; 0\,. \tag{2}$$

Here, θ and $\dot{\theta}$ are the generator rotor angles and frequencies, M and D are the diagonal matrices of generator inertia and damping coefficients, and L is a Laplacian matrix that describes the interactions between generators, see [31]. The swing dynamics (2) feature an inherent *rotational symmetry* and are invariant under a rigid rotation of all angles θ.

The swing dynamics (2) illustrate the cause of inter-area oscillations: the swing equations describe a large-scale system of heterogenous oscillators harmonically (with distinct inertia and damping coefficients) coupled through a spring-type network with Laplacian matrix L. Inter-area oscillations arise from modular network topologies and weights (encoded in the Laplacian matrix L) featuring densely connected groups of generators (so-called areas), which are sparsely connected among another. These areas can be aggregated into coherent groups of machines which swing relative to each other; see the slow coherency analysis in [18], [19].

In this paper, we design wide-area controllers to suppress such inter-area oscillations. With a linear static state feedback $u = -Gx$ (to be designed later), the closed-loop system takes the form

$$\begin{aligned} \dot{x} \;&=\; (A - B_2\,G)\,x \;+\; B_1\,d \\ z \;&=\; \left[\begin{array}{c} z_1 \\ z_2 \end{array}\right] = \left[\begin{array}{c} Q^{1/2} \\ -R^{1/2}\,G \end{array}\right] x \end{aligned} \tag{3}$$

where z is a performance output with state and control weights Q and R. The preceding discussion on inter-area oscillations suggests that homogeneous networks (with identical all-to-all coupling among generators) feature no inter-area oscillations. This suggests a state objective of the form

$$x^T\,Q\,x \;=\; \frac{1}{2}\,\theta^T\,L_{\rm unif}\,\theta \;+\; \frac{1}{2}\,\dot{\theta}^T\,M\,\dot{\theta}.$$

where $L_{\rm unif}$ is the uniform Laplacian (or projector) matrix

$$L_{\rm unif} \;=\; I \;-\; (1/N)\,\mathbb{1}\,\mathbb{1}^T. \tag{4}$$

where $\mathbb{1}$ denotes the vectors of all ones. The objective function x^TQx quantifies the kinetic and potential energy of the swing dynamics in a homogeneous network, and preservers rotational symmetry. The term u^TRu quantifies the control efforts. In summary, the performance output z_1 describes the deviation from a homogenous network without inter-area oscillations. For simplicity, we choose the control weight R to be the identity matrix.

B. Analysis of power spectral density and variance amplification

The conventional analysis of inter-area oscillations is based on spatial profiles of eigenvectors and participation factors of poorly damped modes. Likewise, the traditional control design is also based on a spectral and modal perspective [5], [6]. In this paper, we analyze and control inter-area oscillations from the perspective of power spectral density and output covariance of both the open-loop and the closed-loop system [36]–[38]. This approach offers additional and complementary insights to a modal analysis.

We briefly review the power spectral density and variance amplification analysis of a linear state space system of the form (3). The $\mathcal{H}_2$ norm from the white noise input d to the performance output z is defined as

$$\begin{aligned} \|H(j\omega)\|_2^2 \;&=\; \frac{1}{2\pi}\int_{-\infty}^{\infty} \|H(j\omega)\|_{HS}^2\,d\omega \\ &=\; \mathrm{trace}\,\big(X\,(Q \;+\; G^T\,R\,G)\big) \end{aligned} \tag{5}$$

where $H(j\omega)$ is the transfer function from d to z in the frequency domain, and the controllability Gramian X is the solution to the Lyapunov equation [39]

$$(A - B_2G)\,X \;+\; X\,(A - B_2G)^T \;=\; -B_1\,B_1^T. \tag{6}$$

Here, the Hilbert-Schmidt norm $\|H(j\omega)\|_{HS}^2$ is defined as

$$\begin{aligned} \|H(j\omega)\|_{HS}^2 \;&=\; \mathrm{trace}\,(H(j\omega)\,H^*(j\omega)) \\ &=\; \sum_i \sigma_i^2(H(j\omega)), \end{aligned} \tag{7}$$

where the σ_i's are the singular values of $H(j\omega)$. The Hilbert-Schmidt norm quantifies the power spectral density of the stochastically forced system (3).

The controllability Gramian X in (6) is also the state covariance matrix, and

$$Y \;=\; Q^{1/2}XQ^{1/2}$$

is the output covariance matrix corresponding to z_1. The

eigenvalue decomposition of the output covariance matrix

$$Y \;=\; \sum_i \lambda_i \, v_i \, v_i^T \tag{8}$$

provides insight about the spatial distribution of modes that determine variance amplification. Here, λ_i's and v_i's are the eigenvalues and right eigenvectors of the matrix Y.

C. Sparsity-promoting linear quadratic control with structural constraints

The sparsity-promoting optimal control framework developed in [24] aims at finding a static state feedback G that simultaneously optimizes the $\mathcal{H}_2$ norm of system (3) while inducing a sparse control architecture. Compared to conventional optimal control and stabilization problems, as a result of the rotational symmetry, both the open-loop matrix A and the state performance weight Q feature a common zero eigenvalue with identical eigenvector associated with the average of all rotor angles. In earlier work [30], [31], to arrive at a stabilizing and numerically feasible solution, we have removed the natural rotational symmetry by adding a small regularization term to the diagonal elements of performance matrix Q. The resulting controllers require the use of absolute angle measurements to stabilize the average rotor angle. Besides the problem of obtaining absolute angle measurements (with respect to a common reference), such a regularization also induces a slack bus (a reference generator with fixed angle) and implicitly manipulates the original network infrastructure.

In this article, we restrict our attention to only relative rotor angle measurements which preserve the natural network symmetries. Note that this requirement imposes structural constraints on the feedback gain G: the average rotor angle has to remain invariant under the state feedback $u = -Gx$. To cope with these structural constraints, we augment the approach in [24]. Considering the following coordinate transformation

$$T \;=\; \begin{bmatrix} U & 0 \\ 0 & I \end{bmatrix},$$

where the columns of matrix $U \in \mathbb{R}^{N\times(N-1)}$ (N is the number of generators) form an orthonormal basis for the subspace $\mathbb{1}^{\perp}$. We can obtain the columns of U from the $(N-1)$ eigenvectors of matrix L_{unif} in (4) corresponding to the non-zero eigenvalues. In the new set of coordinates, the matrices of the closed-loop system (3) change to

$$\bar{A} \;:=\; T^T A\, T, \quad \bar{B}_i \;:=\; T^T B_i, \quad \bar{Q}^{1/2} \;:=\; Q^{1/2}\, T.$$

The feedback matrices G (in the original set of coordinates) and F (in the new set of coordinates) are related by

$$F \;=\; G\, T \quad \Leftrightarrow \quad G \;=\; F\, T^T.$$

The $\mathcal{H}_2$ norm from d to z is then obtained as

$$J(F) \;:=\; \begin{cases} \text{trace}\left(\bar{B}_1^T\, P(F)\, \bar{B}_1\right) & \text{for } F \text{ stabilizing,} \\ \infty & \text{otherwise,} \end{cases}$$

where $P(F)$ is the closed-loop observability Gramian that satisfies the Lyapunov equation

$$(\bar{A} \,-\, \bar{B}_2\, F)^T P \,+\, P\,(\bar{A} \,-\, \bar{B}_2\, F) \;=\; -(\bar{Q} \,+\, F^T \bar{R}\, F).$$

Our objective is to achieve a desirable tradeoff between the $\mathcal{H}_2$ performance of the closed-loop system and the sparsity of the feedback gain. While the $\mathcal{H}_2$ performance is expressed in terms of the feedback matrix F in the new set of coordinates, it is desired to enhance sparsity of the feedback matrix G in the original set of coordinates. In order to achieve this task, we formulate the sparsity-promoting optimal control problem as

$$\begin{aligned} &\text{minimize} && J(F) \;+\; \gamma\, g(G) \\ &\text{subject to} && F\, T^T \;-\; G \;=\; 0 \end{aligned} \tag{9}$$

where $\gamma > 0$ is a design parameter which specifies the emphasis on sparsity, and the regularization term is determined by the weighted ℓ_1-norm of G:

$$g(G) \;:=\; \sum_{i,\,j} W_{ij}\, |G_{ij}|.$$

In [29], we showed how to efficiently solve the optimization problem (9) by an iterative approach utilizing the alternating direction method of multipliers (ADMM) algorithm [24], [40]. Algorithmic details for solving this problem are provided in the appendix.

We are now in a position to design state feedback gains G that maintain rotational symmetry and achieve a desirable tradeoff between variance amplification of the closed-loop system and sparsity of the controller.

III. Case Study: IEEE 39 New England Example

We consider the IEEE 39 New England model, which is illustrated in Fig. 1 and consists of 39 buses and 10 detailed two-axis generator models. Generators 1 to 9 are equipped with excitation control systems, and generator 10 is an equivalent aggregated model representing a neighboring transmission network area.

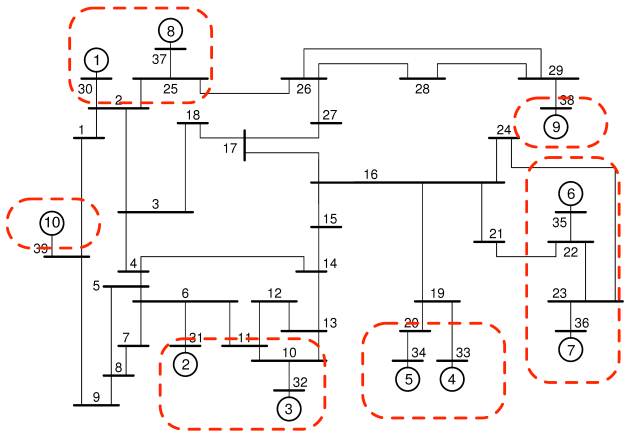

Fig. 1: IEEE 39 New England Power Grid and its groups of coherent machines

We follow a two-level control strategy that combines local and wide-area control. The local control inputs are based on a conventional power system stabilizer (PSS) design to suppress local oscillations, while the wide-area controller is designed to damp inter-area oscillations. For the local control, we use a standard PSS controller with lead/lag elements and carefully tuned coefficients taken from [9]; see [31] for further details. For the subsequent analysis and the wide-area control design, we assume that the local PSS controllers are embedded in the open-loop system matrix A.

A. Open-loop system analysis

Despite the action of the local PSS controllers, a modal analysis of the eigenvalue decomposition and participation factors reveals the presence of five dominant inter-area modes in the open-loop New England power grid model [31]. These modes are reported in Table I, and the groups of coherent machines (identified from the spatial profiles of eigenvectors) are illustrated in Fig. 1. This spatial profile together with modal controllability and observability metrics [13], [14] can be used to indicate which wide-area controller links need to be added to dampen or distort the inter-area modes.

TABLE I: Inter-area modes of the New England power grid

mode no.	eigenvalue pair	damping ratio	frequency [Hz]	coherent groups
1	$-0.6347 \pm \mathrm{i}\,3.7672$	0.16614	0.59956	10 vs. all others
2	$-0.7738 \pm \mathrm{i}\,6.7684$	0.11358	1.0772	1,8 vs. 2-7,9,10
3	$-1.1310 \pm \mathrm{i}\,5.7304$	0.19364	0.91202	1,2,3,8,9 vs. 4-7
4	$-1.1467 \pm \mathrm{i}\,5.9095$	0.19049	0.94052	4,5,6,7,9 vs. 2,3
5	$-1.5219 \pm \mathrm{i}\,5.8923$	0.25009	0.93778	4,5 vs. 6,7

Here, we depart from this modal perspective and follow a different path. We first study the power spectral density and variance amplification of the open-loop system, which identifies the frequencies for which large amplification occurs.

In Fig. 2, the power spectral density of the open-loop system is shown. Observe that the largest amplification occurs for small temporal frequencies, and there are two resonant peaks. The first peak at $\omega_1 = 5.7882$ rad/s corresponds to $f_1 = \omega_1/2\pi = 0.9212$ Hz and is aligned with the inter-area modes $2, 3, 4, 5$ in Table I. the second peak at $\omega_2 = 3.7896$ rad/s corresponds to $f_2 = \omega_2/2\pi = 0.5996$ Hz and is aligned with inter-area mode 1 in Table I.

Next we study the diagonal elements and the eigenvalue decomposition of the output covariance matrix, which shows the contribution of each generator to the variance amplification. In Fig. 3, the diagonal elements of the open-loop output covariance matrix are plotted to show the angle and frequency variance of the individual generators. Fig. 4 displays the eigenvectors corresponding to the four largest eigenvalues of the open-loop output covariance matrix. In Fig. 3 and 4, the first 10 indices correspond to angles and remaining ones correspond to frequencies. From Fig. 3, we observe that frequencies are better aligned than angles. We conclude that the bulk of the variance arises from the misalignment of angles, in particular those of generators 4, 5, 8 and 9. A similar observation can be made from the spatial profile of the eigenvectors in Fig. 4: the largest contribution to the variance amplification is caused by the angle deviation of generators 4, 5, 8 and 9.

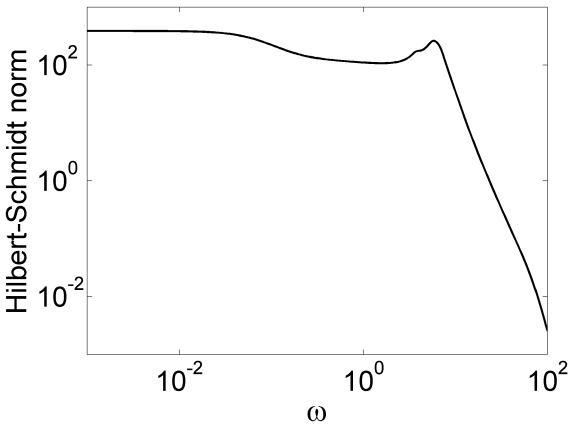

Fig. 2: Power spectral density.

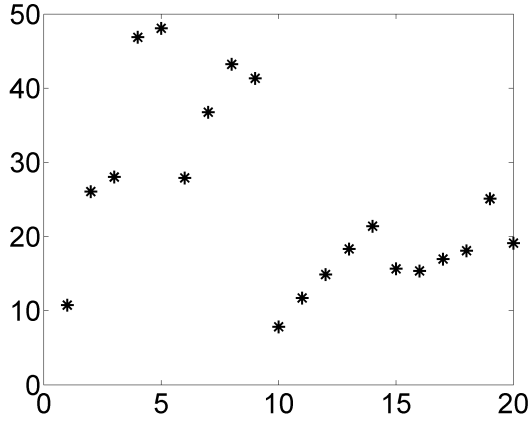

Fig. 3: Open-loop variance.

The diagonal values of the output covariance matrix and the spatial profile of its dominant eigenvalues provide us with a similar understanding as the conventional modal analysis presented in [31]. On the other hand, by looking at the modes corresponding to the dominant eigenvalues of the output covariance matrix, our analysis provides additional insights about the sources of variance amplification. Moreover, our sparsity-promoting $\mathcal{H}_2$ optimal control design is explicitly based on minimizing the output covariance. As a result, this $\mathcal{H}_2$ analysis framework also explains the sparsity pattern of the resulting controllers, for example, why certain long-range communication links are important for the closed-loop performance.

B. Sparsity-promoting optimal control

We used sparsity-promoting optimal control formulation (9) with 100 logarithmically-spaced points for $\gamma = [10^{-4}, 2]$. In Fig. 5, sparsity patterns of the feedback

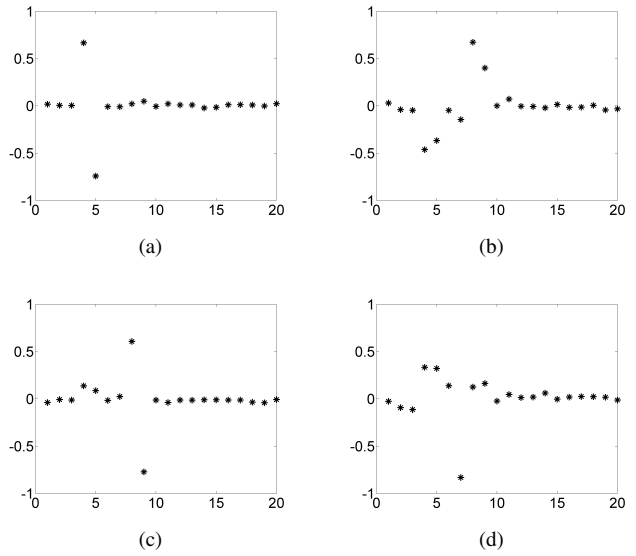

Fig. 4: Eigenvector corresponding to the four largest eigenvalues of the covariance matrix Y of the open-loop system.

matrix G for different values of γ are illustrated. When $\gamma = 0.1099$, controller on generator 9 needs to have access to the rotor angles of generator 5 and the aggregated model 10. This wide-area control architecture is not surprising since generator 9 is the least connected generator (in terms of the effective resistance metric, see [41]), the aggregated model 10 dominates[1] the power system's kinetic energy $1/2\ \dot{\theta}^T M \dot{\theta}$, and generator 5 dominates the most energetic coherent group consisting of generators 4 and 5 (see the spatial distribution in Fig. 3 and 4) in terms of kinetic energy. For $\gamma = 0.4460$, we obtain a fully-decentralized controller, and performance is compromised by about 7.5% relative to the optimal centralized controller; see Fig. 6. By increasing γ to 2, the performance is compromised by about 10.5%.

We emphasize that we can embed our fully decentralized controller into the local generator excitation control systems, for example, by directly feeding the decentralized and local state-feedback to the automatic voltage regulator or by retuning the gains of the existing local PSS controllers. In other words, inter-area oscillations can be suppressed by purely local control strategies while achieving nearly the same performance of the optimal centralized controller [39].

C. Comparison of open-loop and closed-loop systems

The structure of the sparsity-promoting controller with $\gamma = 2$ is shown in Fig. 5c. This controller is fully decentralized with only 18 nonzero elements. In this section, we compare the power spectral density and variance amplification of the following three systems: the open-loop system, the closed-loop system with optimal centralized controller,

[1]The inertia of the aggregated equivalent model 10 is an order of magnitude larger than those of the physical generators $1, \ldots, 9$.

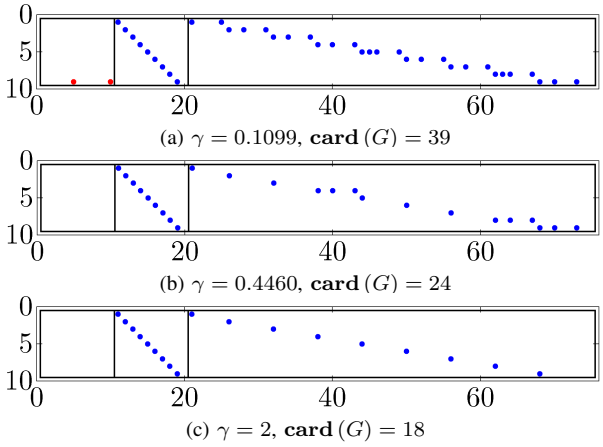

Fig. 5: Sparsity pattern of G.

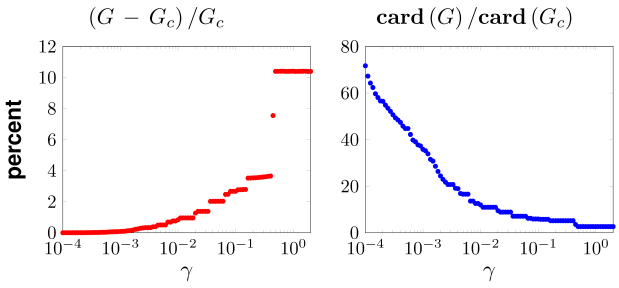

Fig. 6: Performance vs sparsity.

and the closed-loop system with the sparse decentralized controller depicted in Fig. 5c.

Fig. 7 provides a comparison between the power spectral densities of three cases. The fully decentralized sparse controller performs almost as well as the optimal centralized controller for high frequencies; for low frequencies, we observe some discrepancy that accounts for about $10\,\%$ of performance degradation in the variance amplification.

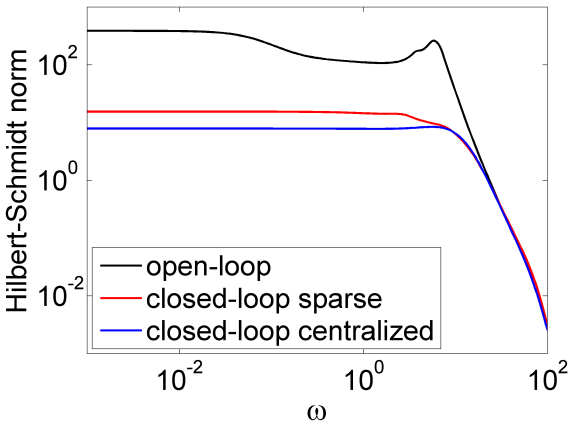

Fig. 7: Power spectral density comparison.

In Fig. 8, we plot the eigenvalues of the output covariance matrix Y to demonstrate the variance amplification of both kinetic and potential energy for the three cases. It can be observed that the optimal centralized as well as the decentralized feedback do not only lower the variance amplification of the open-loop system, but they also balance the spectrum, i.e. they equalize the variance amplification of all modes. The diagonal elements of the output covariance

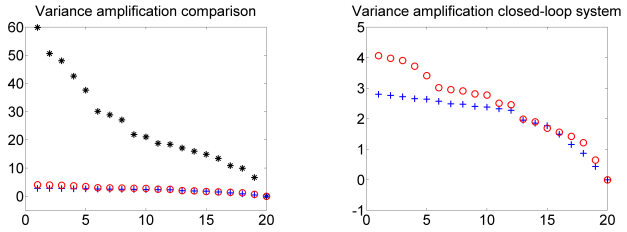

Fig. 8: Variance amplification comparison. $*$'s represent open-loop system, $\circ$'s represent closed-loop system with sparse decentralized controller and $+$'s represent closed-loop system with optimal centralized controller.

matrix for all three cases are shown in Fig. 9. We observe that our control strategy is capable of diminishing the variance of both angles and frequencies. Additionally, the diagonal elements of the output covariance matrix are also equalized and balanced both by the optimal centralized and the decentralized controller. We conclude that, similar to the modal observations discussed in [31], the optimal feedback gain not only increases the damping of the eigenvalues associated with the inter-area modes, but it structurally distorts these modes by rotating the corresponding eigenvectors.

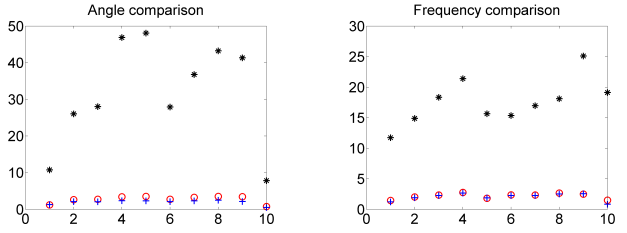

Fig. 9: Angle and frequency variance.

IV. Concluding Remarks

In this paper, we analyzed inter-area oscillations of power systems by studying their power spectral density functions and output covariance matrices. Our open-loop analysis identifies the generators that contribute most to the inter-area oscillations. By comparing open-loop and closed-loop systems, we are able to understand the effect of the sparsity-promoting control both in terms of performance and with regards to the resulting closed-loop communication pattern.

APPENDIX

A. Sparsity-promoting optimal control algorithm

We briefly summarize the alternating direction method of multiplier (ADMM) algorithm in the sparsity-promoting optimal control design approach introduced in Section III to solve (9). We refer readers to [24] for additional details. The algorithms and examples used in this paper have been implemented in *Matlab* and can be downloaded at `www.ece.umn.edu/users/mihailo/software/lqrsp/`.

1) Augmented Lagrangian: First, we form augmented Lagrangian associated with the constrained problem (9)

$$\mathcal{L}_\rho(F,G,\Lambda) \;=\; J(F) \;+\; \gamma\, g(G) \;+\; \mathrm{trace}\left(\Lambda^T(F\,T^T \;-\; G)\right) \;+\; \frac{\rho}{2}\,\|\,F\,T^T - G\,\|_F^2$$

where Λ denotes the matrix of Lagrange multipliers and $\|\cdot\|_F$ is the Frobenius norm of a matrix. The positive regularization parameter γ specifies the importance of sparsity. For $\gamma = 0$, the standard centralized linear quadratic regulator is obtained; as γ increases, the feedback matrix G becomes increasingly sparser.

2) Iterative ADMM algorithm: Next, we use a sequence of iterations following the ADMM algorithm to find a minimizer of the constrained problem (9)

$$\begin{aligned} F^{k+1} &= \arg\min_F \mathcal{L}_\rho\,(F,\,G^k,\,\Lambda^k) \\ G^{k+1} &= \arg\min_G \mathcal{L}_\rho\,(F^{k+1},\,G,\,\Lambda^k) \\ \Lambda^{k+1} &= \Lambda^k + \rho\,(F^{k+1}\,T^T - G^{k+1}). \end{aligned}$$

In contrast to the general method of multipliers, in which we minimize F and G jointly, ADMM separates the problem into an F-minimization step which can be solved using descent method, a G-minimization step and a dual variable update step, that have analytical solutions.

3) Stopping criterion:

$$\begin{aligned} \|F^{k+1}\,T^T - G^{k+1}\| &\le \epsilon \\ \|G^{k+1} - G^k\| &\le \epsilon \end{aligned}$$

The ADMM algorithm stops when both primal and dual residuals are smaller than the pre-specified thresholds.

4) Polishing step: Finally, we fix the sparsity pattern of G identified using ADMM and solve the optimal control problem with structural constraints corresponding to the identified controller architecture.

References

[1] F. Alvarado, C. DeMarco, I. Dobson, P. Sauer, S. Greene, H. Engdahl, and J. Zhang, "Avoiding and suppressing oscillations," *PSERC Project Final Report*, 1999.

[2] V. Venkatasubramanian and Y. Li, "Analysis of 1996 Western American electric blackouts," in *Bulk Power System Dynamics and Control-VI*, Cortina d'Ampezzo, Italy, 2004.

[3] K. Prasertwong, N. Mithulananthan, and D. Thakur, "Understanding low-frequency oscillation in power systems," *International Journal of Electrical Engineering Education*, vol. 47, no. 3, pp. 248–262, 2010.

[4] L. Rouco, "Eigenvalue-based methods for analysis and control of power system oscillations," in *Power System Dynamics Stabilisation, IEE Colloquium on*. IET, 1998.

[5] G. Rogers, "Demystifying power system oscillations," *Computer Applications in Power, IEEE*, vol. 9, no. 3, pp. 30–35, 1996.

[6] M. Klein, G. Rogers, and P. Kundur, "A fundamental study of inter-area oscillations in power systems," *Power Systems, IEEE Transactions on*, vol. 6, no. 3, pp. 914–921, 1991.

[7] M. Klein, G. Rogers, S. Moorty, and P. Kundur, "Analytical investigation of factors influencing power system stabilizers performance," *Energy Conversion, IEEE Transactions on*, vol. 7, no. 3, pp. 382–390, 1992.

[8] N. Martins and L. T. G. Lima, "Eigenvalue and frequency domain analysis of small-signal electromechanical stability problems," in *IEEE/PES Symposium on Applications of Eigenanalysis and Frequency Domain Methods*, 1989, pp. 17–33.

[9] R. A. Jabr, B. C. Pal, N. Martins, and J. C. R. Ferraz, "Robust and coordinated tuning of power system stabiliser gains using sequential linear programming," *IET Generation, Transmission & Distribution*, vol. 4, no. 8, pp. 893–904, 2010.

[10] J. Xiao, F. Wen, C. Y. Chung, and K. P. Wong, "Wide-area protection and its applications-a bibliographical survey," in *IEEE PES Power Systems Conference and Exposition*, Atlanta, GA, USA, Oct. 2006, pp. 1388–1397.

[11] K. Seethalekshmi, S. N. Singh, and S. C. Srivastava, "Wide-area protection and control: Present status and key challenges," in *Fifteenth National Power Systems Conference*, Bombay, India, Dec. 2008, pp. 169–175.

[12] M. Amin, "Special issue on energy infrastructure defense systems," *Proceedings of the IEEE*, vol. 93, no. 5, pp. 855–860, 2005.

[13] A. Heniche and I. Karnwa, "Control loops selection to damp inter-area oscillations of electrical networks," *IEEE Transactions on Power Systems*, vol. 17, no. 2, pp. 378–384, 2002.

[14] L. P. Kunjumuhammed, R. Singh, and B. C. Pal, "Robust signal selection for damping of inter-area oscillations," *IET Generation, Transmission & Distribution*, vol. 6, no. 5, pp. 404–416, 2012.

[15] G. E. Boukarim, S. Wang, J. H. Chow, G. N. Taranto, and N. Martins, "A comparison of classical, robust, and decentralized control designs for multiple power system stabilizers," *IEEE Transactions on Power Systems*, vol. 15, no. 4, pp. 1287–1292, 2000.

[16] Y. Zhang and A. Bose, "Design of wide-area damping controllers for interarea oscillations," *IEEE Transactions on Power Systems*, vol. 23, no. 3, pp. 1136–1143, 2008.

[17] M. Zima, M. Larsson, P. Korba, C. Rehtanz, and G. Andersson, "Design aspects for wide-area monitoring and control systems," *Proceedings of the IEEE*, vol. 93, no. 5, pp. 980–996, 2005.

[18] J. H. Chow and P. Kokotović, "Time scale modeling of sparse dynamic networks," *IEEE Transactions on Automatic Control*, vol. 30, no. 8, pp. 714–722, 1985.

[19] D. Romeres, F. Dörfler, and F. Bullo, "Novel results on slow coherency in consensus and power networks," in *European Control Conference*, Zürich, Switzerland, July 2013, to appear.

[20] B. Bamieh, M. R. Jovanović, P. Mitra, and S. Patterson, "Coherence in large-scale networks: dimension dependent limitations of local feedback," *IEEE Trans. Automat. Control*, vol. 57, no. 9, pp. 2235–2249, September 2012.

[21] B. Bamieh and D. F. Gayme, "The price of synchrony: Resistive losses due to phase synchronization in power networks," 2012.

[22] M. Fardad, F. Lin, and M. R. Jovanović, "Design of optimal sparse interconnection graphs for synchronization of oscillator networks," *IEEE Trans. Automat. Control*, 2013, submitted; also arXiv:1302.0449.

[23] S. Schuler, U. Münz, and F. Allgöwer, "Decentralized state feedback control for interconnected process systems," in *IFAC Symposium on Advanced Control of Chemical Processes*, Furama Riverfront, Singapore, July 2012, pp. 1–10.

[24] F. Lin, M. Fardad, and M. R. Jovanović, "Design of optimal sparse feedback gains via the alternating direction method of multipliers," *IEEE Trans. Automat. Control*, vol. 58, no. 9, pp. 2426–2431, September 2013.

[25] F. Lin, M. Fardad, and M. R. Jovanović, "Sparse feedback synthesis via the alternating direction method of multipliers," in *Proceedings of the 2012 American Control Conference*, Montréal, Canada, 2012, pp. 4765–4770.

[26] M. Fardad, F. Lin, and M. R. Jovanović, "Sparsity-promoting optimal control for a class of distributed systems," in *Proceedings of the 2011 American Control Conference*, San Francisco, CA, 2011, pp. 2050–2055.

[27] S. Schuler, U. Münz, and F. Allgöwer, "Decentralized state feedback control for interconnected systems with application to power systems," *Journal of Process Control*, 2013, in press.

[28] U. Münz, M. Pfister, and P. Wolfrum, "Sensor and actuator placement for linear systems based on H_2 and H_∞ optimization," 2013, submitted.

[29] X. Wu and M. R. Jovanović, "Sparsity-promoting optimal control of consensus and synchronization networks," in *American Control Conference*, 2013, submitted.

[30] F. Dörfler, M. R. Jovanović, M. Chertkov, and F. Bullo, "Sparse and optimal wide-area damping control in power networks," in *American Control Conference*, Washington, DC, USA, June 2013, pp. 4295–4300.

[31] F. Dörfler, M. R. Jovanović, M. Chertkov, and F. Bullo, "Sparsity-promoting optimal wide-area control of power networks," *IEEE Trans. Power Syst.*, 2013, submitted; also arXiv:1307.4342.

[32] B. E. Eliasson and D. J. Hill, "Damping structure and sensitivity in the NORDEL power system," *IEEE Transactions on Power Systems*, vol. 7, no. 1, pp. 97–105, 1992.

[33] J. H. Chow and K. W. Cheung, "A toolbox for power system dynamics and control engineering education and research," *IEEE Transactions on Power Systems*, vol. 7, no. 4, pp. 1559–1564, 1992.

[34] P. Kundur, *Power system stability and control*. McGraw-Hill, 1994.

[35] P. M. Anderson and A. A. Fouad, *Power system control and stability*. Wiley, 2008.

[36] P. Stoica and R. L. Moses, *Introduction to spectral analysis*. Prentice Hall, 1997, vol. 1.

[37] D. B. Leeson, "A simple model of feedback oscillator noise spectrum," *Proceedings of the IEEE*, vol. 54, no. 2, pp. 329–330, 1966.

[38] R. Martin, "Noise power spectral density estimation based on optimal smoothing and minimum statistics," *IEEE Transactions on Speech and Audio Processing*, vol. 9, no. 5, pp. 504–512, 2001.

[39] J. P. Hespanha, *Linear systems theory*. Princeton University Press, 2009.

[40] S. Boyd, N. Parikh, E. Chu, B. Peleato, and J. Eckstein, "Distributed optimization and statistical learning via the alternating direction method of multipliers," *Foundations and Trends in Machine Learning*, vol. 3, no. 1, pp. 1–124, 2011.

[41] F. Dörfler and F. Bullo, "Kron reduction of graphs with applications to electrical networks," *IEEE Transactions on Circuits and Systems I: Regular Papers*, vol. 60, no. 1, pp. 150–163, 2013.